

Synthesis, Characterization, and *In-Vitro* Evaluation of Silibinin-loaded PEGylated Niosomal Nanoparticles: Potential Anti-Cancer Effects on SW480 Colon Cancer Cells

Urjwan Alali¹, Maha Mohammed Kadhim Al-Tu'ma², Ammar Fadhil Jawad³, Saja Talib Ahmed⁴, Hanaa Addai Ali⁴, Siham Abdulzehra⁵, Fadhil Jawad Al-Tu'ma^{6*}

Abstract

Objective: Colorectal cancer is a significant global health concern with high mortality rates. Silibinin is a compound derived from milk thistle with anticancer properties and may be a potential treatment option for colorectal cancer. Its poor solubility limits its clinical application, but various strategies, such as nanoparticle encapsulation, have shown promise. In this study, a PEGylated niosomal drug delivery system was used to enhance the solubility of silibinin, and its anti-proliferative effects were evaluated against human colorectal cancer cell lines. **Methods:** The silibinin-loaded PEGylated niosomal nanoparticles (NIO-SIL) were fabricated using the thin-film hydration method and characterized with dialysis bag, AFM, SEM, DLS, and FTIR systems. Finally, the cancerous cells and human normal cells were treated with NIO-SIL and pure silibinin. The proliferation, apoptosis, and cell cycle of these cells were evaluated. Subsequently, the expression of *Bax*, *Bcl-2*, *p53*, and cyclin D1 genes was measured using real-time PCR. **Result:** The drug release profile, size, morphology, and chemical interactions of the synthesized PEGylated niosomal nanoparticles were suitable for use as a drug delivery system. Both pure silibinin and NIO-SIL could reduce the proliferation of cancerous cells, induce apoptosis, and cause cell cycle arrest, with no significant negative effects reported on human normal cells. Both pure silibinin and NIO-SIL reduced the expression of the *Bcl-2* and cyclin D1 genes while increasing the expression of *Bax* and *p53*. (p-value < 0.05 *). **Conclusion:** The outcomes of this study indicate the high potential of PEGylated niosomal nanoparticles for encapsulation and delivery of silibinin to cancer cells, with no negative effects on normal cells.

Keywords: Colorectal cancer- Silibinin- Niosome- Nanoparticle- PEGylated

Asian Pac J Cancer Prev, 25 (7), 2539-2550

Introduction

Colorectal cancer is a significant public health concern and one of the most prevalent cancers with high fatality rates [1]. The incidence of colon cancer has been rapidly increasing in recent decades in Asian countries, making it the third most common cause of cancer-related deaths in Korea [2]. In 2020, 1.15 million new cases of colon cancer were reported globally, accounting for about 60% of all colorectal cancer cases [3]. Additionally, there has been an increase in the prevalence of cancers (3.3% to 11.1% depending on types) among diagnosed individuals with colorectal cancer [4].

The examination of cancer at a cellular level has

uncovered chromosomal instability as a critical factor linked to disease progression and survival outcomes [5]. Detailed analysis focusing on alterations in DNA copy numbers has revealed that over 85% of cancers exhibit chromosomal abnormalities, emphasizing how crucial chromosomal instability is, within this particular type of cancer [6]. Moreover, the presence and activity of proteins, for repairing DNA double strand breaks, ATM and BRCA1 have been associated with predicting the likelihood of survival in individuals with colorectal cancer. This connection highlights the significance of instability, in influencing patient outcomes [7]. Additionally, the study highlighted the occurrence of chromosomal aberrations in colorectal tumors, further underlining the role of

¹Department of Pharmaceutical Chemistry, College of Pharmacy, University of Kerbala, Kerbala, Iraq. ²Department of Anesthesia Techniques, College of Health and Medical Techniques, Al-Zahraa University for Women, Kerbala, Iraq. ³Department of Pharmacognesy, College of Pharmacy, University of Kerbala, Kerbala, Iraq. ⁴Department of Chemistry, College of Science, University of Kufa, Kufa, Iraq. ⁵Department of Clinical Biochemistry and Laboratory Medicine, Faculty of Medicine, Tabriz University of Medical Sciences, Tabriz, Iran. ⁶Department of Chemistry and Biochemistry, College of Medicine, University of Kerbala, Kerbala, Iraq. *For Correspondence: fadhil.jawad.altuma@gmail.com

chromosomal instability in the pathogenesis of colorectal cancer [8].

Silibinin, extracted from the seeds of milk thistle (*Silybum marianum*), is a component of silymarin [9]. It possesses a range of activities, including antioxidant, anti-inflammatory and antineoplastic effects [10]. Silibinin has been utilized for years in treating diseases like early phase hepatocirrhosis and fatty liver [11]. Moreover, it shows promising potential as a cancer therapy by combating tumor chemoresistance across various cancer types [12]. Research has demonstrated that silibinin exhibits antineoplastic properties, making it a potential candidate for cancer treatment [13, 14]. Studies have revealed its ability to induce apoptosis and inhibit cell proliferation in cancer cell lines, such as lung, gastric, breast, and oral cancers [15-17]. Furthermore, silibinin has demonstrated its ability to enhance the efficacy of anticancer drugs like nintedanib while overcoming tumor cell resistance to specific treatments [14].

However, the poor solubility of silibinin in aqueous environments is a major obstacle in its clinical application [18]. To address this limitation effectively and improve its bioavailability extensive research has focused on formulation strategies for enhancing the solubility of drugs [19, 20]. Numerous research studies have investigated the use of nanoparticles and micelles to enhance the solubility and targeted delivery of silibinin [21, 22]. For instance, Hossainzadeh et al. demonstrated the encapsulation of silibinin in polymersome nanoparticles to overcome its low solubility and enhance its delivery to cancerous cells [22].

Niosomes are a novel drug delivery system that has gained attention due to their potential for sustained, controlled, and targeted medication delivery with high stability [23]. Niosomes are similar structures to liposomes. However, their composition differs as they are formed from ionic surfactants and cholesterol [24]. Niosomes have shown potential in improving the solubility and availability of drugs [25]. For example, niosomes have been investigated for the in vitro delivery of SIL, resulting in improved in vitro dissolution profiles compared to aqueous suspensions [26].

PEGylation is a commonly used technique in drug delivery systems. It involves attaching polyethylene glycol (PEG) to biomolecules and nanoparticles [27]. PEGylation has been successful, in enhancing drug delivery systems by increasing protein stability, prolonging shelf life, and maintaining bioactivity [28]. The utilization of PEGylated nanocarriers has demonstrated promising outcomes in enhancing drug delivery efficiency, reducing toxicity risks, and extending the lifespan of drugs within the bloodstream [29].

PEGylated niosomes have gained attention as potential drug delivery systems due to their ability to improve stability and circulation half-life of drugs [30]. Studies have shown that PEGylated niosomes can serve as effective vehicles for the simultaneous delivery of different chemotherapy agents, exhibiting synergistic interactions to enhance antitumor efficacy [31].

In this research, silibinin was employed as an anti-cancer agent targeting human colorectal cancer cells.

Our investigation encompassed the assessment of cell proliferation and analyzing the expression of key cancer-related genes, including *bax*, *bcl-2*, and *p53*. To address the challenge of silibinin's limited solubility, we developed a PEGylated-niosomal nanoparticle (NPs) system for enhanced delivery.

Materials and Methods

Synthesis of PEGylated niosomal NPs

The PEGylated niosomal nanoparticles (blank NIO) were prepared using the thin film hydration method in combination with sonication. Briefly, a mixture of Span 60, cholesterol, and PEG (in a 1:2:1 ratio) were dissolved in chloroform (3 mL) and methanol (6 mL), and the solvent was evaporated under reduced pressure (0.46 atm) at 60 °C using a rotary evaporator. Hydration of the film was performed by adding 10 ml of phosphate-buffered saline (PBS, pH 7.4) to the round-bottomed flask. The flask was then placed in the water bath shaker set at 100 rpm and 60 °C. Then, probe sonication was applied with an amplitude set at 40% for 15 cycles of two minutes each, with a 30-second rest in between. The fabricated blank NIO was stored at 4°C for future use [25].

Preparation of stock silibinin and silibinin-loaded PEGylated niosomal NPs

The stock solution of silibinin (pure silibinin) was prepared by dissolving 4.8 mg of silibinin in 10 mL of RPMI (containing 10% FBS and 0.05% DMSO) under continuous stirring for 1 h at 25°C. The same steps as above were repeated to fabricate silibinin-loaded PEGylated niosomal nanoparticles (NIO-SIL), except that in the first step, 4.8 mg of silibinin was dissolved in chloroform and methanol along with Span 60, cholesterol, and PEG [32].

Characterization of blank NIO and NIO-SIL

Dynamic light scattering (DLS) was utilized to assess the mean size and surface charge of the fabricated liposomal nanoparticles. The niosomal samples were appropriately diluted (1:10) with PBS, and the dimensions and zeta potential of the samples were measured with Zeta sizer Nano ZS (Malvern Instruments Ltd., Malvern, UK) employing helium–neon laser at 630 nm at 24 °C. The morphology and microstructure of synthesized blank NIO and NIO-SIL NPs were studied using a scanning electron microscopy (SEM) system (MIRA3 TESCAN, Czech). Briefly, the fabricated blank NIO and NIO-SIL NPs rinsed twice with PBS, followed by freeze-drying (Dena Vacuum, FD-5005-BT, Iran) and subsequent scanning using an electron microscope. The interactions at functional groups of Span 60, cholesterol, PEG, and silibinin in blank NIO and NIO-SIL samples were determined using a Fourier transform infrared spectrophotometer (FT-IR Tensor 27 spectrometer). The infrared spectra were scanned in a frequency range between 500 and 4000 cm^{-1} .

Silibinin entrapment efficiency

Following the separation of the fabricated NIO-SIL NPs using the ultracentrifugation technique, the entrapment

efficiency (%) was determined by comparing the total entrapped SIL content within the NIO-SIL NPs with the pure silibinin in the supernatant. The concentration of pure silibinin in the supernatant was detected using UV spectrophotometry (PerkinElmer instrument, Fremont, CA, USA) at 288 nm (λ_{max} of silibinin) [33]. The calculation of entrapment efficiency (EE) percentage was performed as follows:

$$EE\% = \frac{\text{Silibinin in niosomal NPs}}{\text{Initial silibinin}} \times 100\%$$

Silibinin release rate from NIO-SIL NPs

A Dialysis bag (with a molecular weight cutoff of 12–14 KD) containing 1 ml of NIO-SIL NPs was immersed in PBS buffers with pH levels of 5.2 and 7.4. The buffer magnetically stirred at 150 rpm at 37 °C. At specified intervals, 2 ml of the leaked solution exchanged with same amount of fresh PSB. The concentration of the silibinin was subsequently assessed spectrophotometrically (PerkinElmer instrument, Fremont, CA, USA) at 288 nm. The percentage of released silibinin was calculated by determining the ratio of the released amount of silibinin in the dialysis bag to the total silibinin [26].

Cancerous and normal cell culture

Human normal cell line (HEK-293) and human colon carcinoma (SW480) cells were purchased from the Institute Pasteur of Iran and cultured in T75 flasks containing RPMI (Gibco, Hong Kong, China), supplemented with fetal bovine serum (10% FBS, v/v), 10 µg/ml of streptomycin (Sigma, Germany), and 10 U/ml of penicillin (Sigma, Germany) at 37 °C in 5% CO₂ atmosphere [25].

In-vitro cytotoxicity study

SW480 and HEK-293 cells were seeded into 96-well plates (104 cells per well) containing RPMI-1640 medium (with 1% penicillin-streptomycin and 10% FBS) and incubated for 24 hours at 37°C in a 5% CO₂ atmosphere. Cells were treated with different concentrations of NIO-SIL (0, 25, 50, 100, 150, and 200 µM) and pure silibinin (0, 25, 50, 100, 150, and 200 µM) for 48 hours under the same conditions. 100 µL of MTT was added to the treated cell medium and incubated for 4 hours. The supernatant was removed, and 100 µL of DMSO was added to dissolve the formazan crystals generated by the living cells. Finally, the absorbance of the samples was measured using an EL × 800 Microplate Absorbance Reader (Bio-Tek Instruments) at 570 nm. The rate of cytotoxicity was calculated by comparing the absorbance of treated cells with that of untreated cells.

Gene expression study

Cancerous cells (1 × 10⁶) were seeded in each well of a 6-well plate and incubated for 24 hours at 37°C in a 5% CO₂ atmosphere. The cells were exposed to NIO-SIL and pure silibinin at their IC₅₀ concentrations for 48 hours. Afterward, an RNeasy Mini kit (Qiagen) was used to extract total RNA from cells following the manufacturer's instructions. The first-strand cDNA was

synthesized using the RevertAid™ First-Strand cDNA Synthesis Kit (Thermo Fisher Scientific) according to the kit's instructions. QRT-PCR was performed using a SYBR Green Real-time PCR master mix (Primer Design, UK) with a total volume of 20 µL on an ABI 7500 detection system (Applied biosystems) and the following primers (forward and reverse) were used:

GAPDH	5'-GCGCCCAATACGACCAATC-3'
	5'-GCGCCCAATACGACCAATC-3'
Bax	5'-CCAGAGGCGGGTTCAT-3'
	5'-TGTCCAGCCCATGATGGTTC-3'
Bcl-2	5'-AAAAATACAACATCACAGAGGAAGT-3'
	5'-TCCCGGTTATCGTACCCTGT-3'
p53	5'-AAGTCTAGAGCCACCGTCCA-3'
	5'-ACCATCGCTATCTGAGCAGC-3'
Cyclin D1	5'-GACACCTAGTGCCACGGAAA-3'
	5'-AAAGGATAACACGGGGCAGG-3'

Expressions of selected genes were normalized to the GAPDH gene [34].

Apoptosis analysis

A 6-well plate was used for cell culture with an initial seeding of 104 cells. Followed treatments involving NIO-SIL and pure silibinin for a duration of 48 hours. The apoptosis profile was assessed using the Annexin V-FITC Apoptosis Detection Kit (Beyotime, Biotechnology Co., Ltd., Nantong, China). The cells were detached using trypsin (Sigma, Germany), washed with PBS, subjected to centrifugation at 1,500 g for 5 minutes, and the supernatant was discarded. Subsequently, the pellet was resuspended in 500 µL of 1× binding buffer. The resulting solution was treated with 5 µL of Annexin V-FITC and 5 µL of PI, followed by transfer to FACS tubes after thorough mixing and a 15-minute incubation in the dark. Finally, the samples were analyzed using the FACSCalibur Flow Cytometer (FACSCalibur, BD Biosciences, USA). The experimental procedure was repeated three times [35].

Cell cycle analysis

Initially, 1 × 10⁶ cancerous cells were seeded per well in 6-well plates and allowed to attach by incubation for 24 hours. Subsequently, the cells underwent treatment with NIO-SIL and pure silibinin at their IC₅₀ concentrations. After 48 hours of incubation, the cells were trypsinized, washed twice with PBS, and then fixed with 70% ethanol, being held at -20 °C overnight. The collected cells were re-suspended in PBS, and a staining solution containing 1 µg/mL RNase and 100 µg/mL PI was added. The cell mixture was transferred to an incubator for 30 minutes at 37°C. The FACSCalibur flow cytometer (FACSCalibur, BD Biosciences, USA) was used to assess the cell cycle.

Statistical analysis

The results were subjected to statistical analysis using Graph Pad Prism 8.4 software. The data is presented as mean ± standard deviation from three independent

experiments. Statistical comparisons between groups were conducted using ANOVA test, with a significance level set at $p < 0.05$.

Results

Nanoparticles have emerged as a highly promising tool in cancer therapy, leveraging their distinctive properties and potential for precise drug delivery to targeted sites [36]. These nanoscale carriers can be designed to selectively bind and target cancer cells, thereby enhancing treatment efficacy while simultaneously modifying undesirable side effects [37]. Nanoparticle-based therapeutics have demonstrated heightened efficacy and improved safety profiles in contrast to conventional anticancer treatments [38]. Their ability to precisely localize within tumors and undergo active cellular uptake contributes significantly to more efficacious treatment outcomes [39]. Niosomes present a promising path in drug delivery for cancer therapy, given their capacity to selectively target cancer cells, prolong treatment duration, moderate side effects, and enhance drug stability [40]. Niosomes, as vesicular structures composed of nonionic surfactants, exhibit the capability to encapsulate both hydrophilic and lipophilic drugs. This characteristic makes them versatile carriers suitable for a diverse range of pharmaceutical compounds [41].

Furthermore, the size of nanoparticles, including niosomes, plays a crucial role in their effectiveness, with smaller particle sizes being optimal for drug delivery to the deep layers of the skin and potentially enhancing therapeutic efficacy [42]. A critical determinant influencing the size of niosomes is the composition of the lipid bilayer. The inclusion of cholesterol has been demonstrated to elevate the particle size of these vesicles. This arises from the membrane-rigidity-inducing property of cholesterol, which diminishes the impact of sonication, thereby facilitating the formation of larger niosomes [43, 44].

In addition to lipid composition, various factors such as sonication time and pH value influences on niosome size notably. Prolonged sonication times exhibit a negative correlation with niosome size, indicating that extended

sonication results in smaller vesicles. This outcome is likely attributed to the disruptive effects of sonication on the lipid bilayer, leading to formation of smaller vesicles [45]. The pH of the environment emerges as another critical factor influencing the stability and size of niosomes [46]. Additionally, the presence of encapsulated substances within niosomes introduces an additional dimension to size [47]. It is noteworthy that the size of niosomes exhibits variability depend on the formulation and preparation method, spanning a range from 100 to 2000 nm [48]. Figure 1 demonstrates the size of blank NIO-SIL NPs (nm) assessed with DLS. A size difference of 26.8 nm is observed between the two nanoparticles, which, according to recent explanations, is related to silibinin loading between the two membranes.

Polydispersity Index (PDI) in nanoparticles is a crucial parameter that indicates the distribution of particle sizes within a sample. A PDI equal to or below 0.3 is typically acceptable, signifying a uniform dispersion of nanoparticles. In the context of niosomes employed in drug delivery, a low PDI value indicates a homogeneous population of vesicles [49, 50]. Table 1. Listed the size, PDI, and zeta potential of blank NIO and NIO-SIL NPs.

Zeta potential serves as a metric for appraising the surface charge of particles or surfaces within a liquid medium, constituting a crucial parameter in various fields, including colloid science, materials science, and biology [51]. Several factors, such as the composition of the vesicles, the presence of additives, and the pH of the medium, can influence the zeta potential of niosomes [52, 53]. The zeta (ζ)-potential of blank NIO NPs was -26.1 mV, while NIS-SIL NPs had a significantly higher ζ -potential of -39.4 ± 7.6 mV (Table 1).

The morphology of NPs is another important aspect that influences their properties, applications, and interactions with biological systems. For example, the

Table 1. Physical Properties Including Zeta-Potential, Polydispersity Index, and particle size of blank niosome and silibinin-loaded PEGylated niosome NPs.

Sample	PDI	Zeta-potential (mV)	Size by DLS (nm)
Blank NIO	124±7.24	-26.1±4.7	0.546
NIO-SIL	150.8±27.6	-39.4±7.6	1

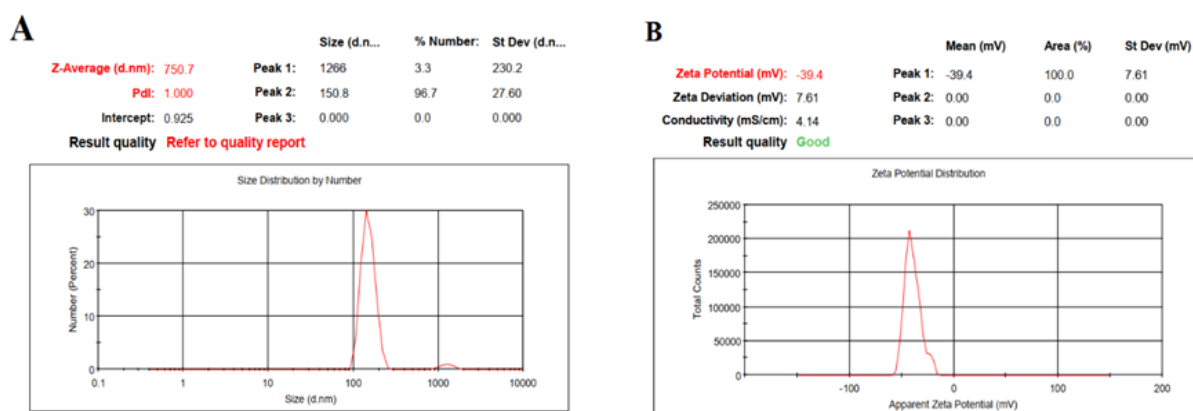


Figure 1. The Dynamic Light Scattering (DLS) Analysis of NIO-SIL Nanoparticles Revealed an Average Diameter Size of 150.8 nm (A), and a Zeta Potential of -39.4 mV for These Nanoparticles (B).

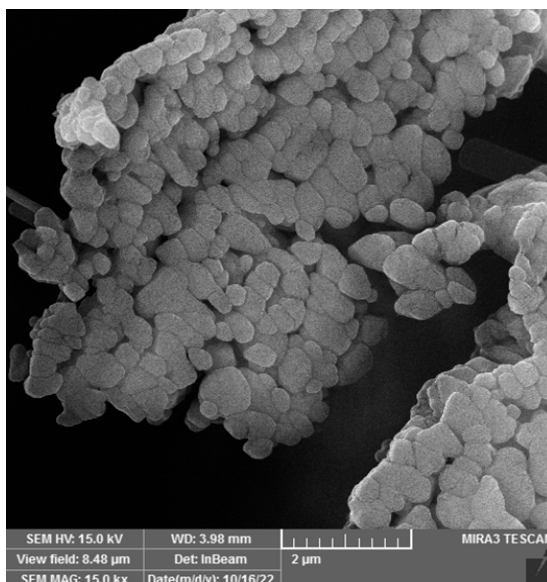


Figure 2. Field Emission Scanning Electron Microscopy (FE-SEM) Image of the Surface Morphology of NIO-SIL NPs Showed a Spherical Morphology.

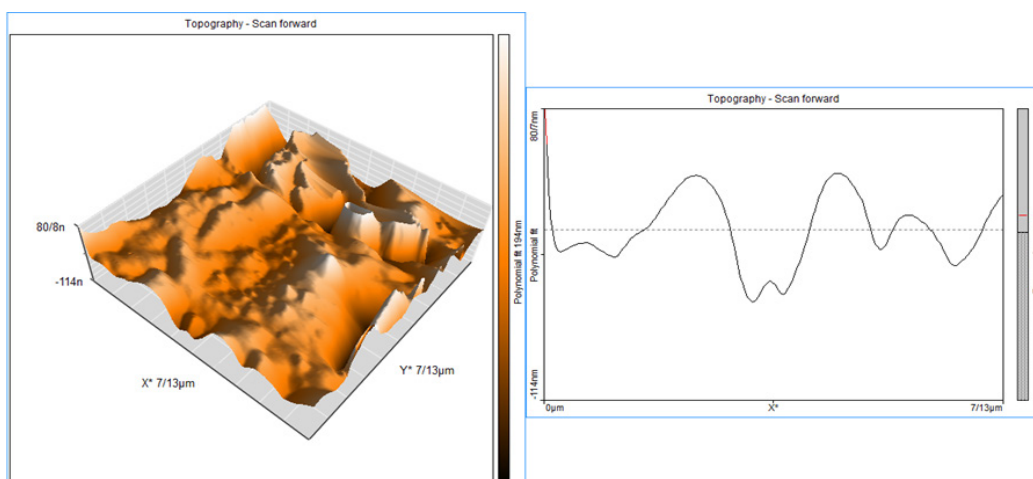


Figure 3. The AFM Image of NIO-SIL NPs Confirmed Previously Obtained Data about These NPs Using SEM.

morphology of nanoparticles can impact their cellular uptake, biodistribution, and toxicity [54]. Based on the

previous studies, it is evident that niosomes exhibit a spherical morphology [55]. Figure 2 shows the

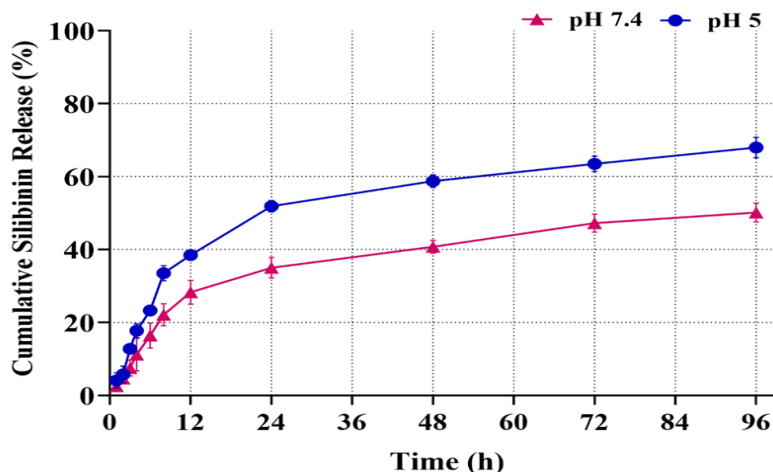


Figure 4. The Cumulative Release Profile of Silibinin in pH 7.4 and 5 from the PEGylated Niosomal NPs (An Initial Burst Release Followed by the Gradual Release). The data are presented as mean \pm SD (n = 3).

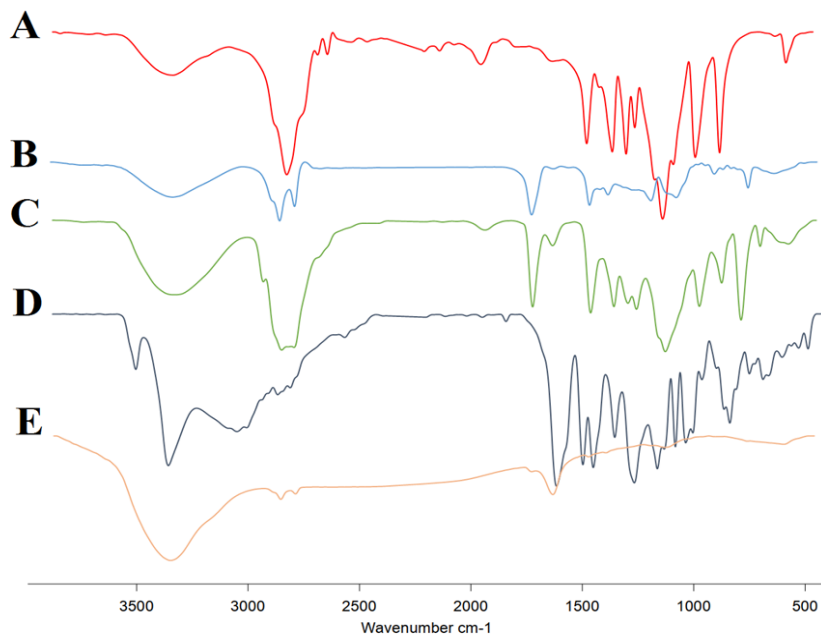


Figure 5. FTIR spectra of (A) PEG, (B) blank NIO NPs, (C) PEG-NIO, (D) silibinin, and (E) NIO-SIL. The spectra indicate the encapsulation of silibinin in the PEGylated niosome NPs.

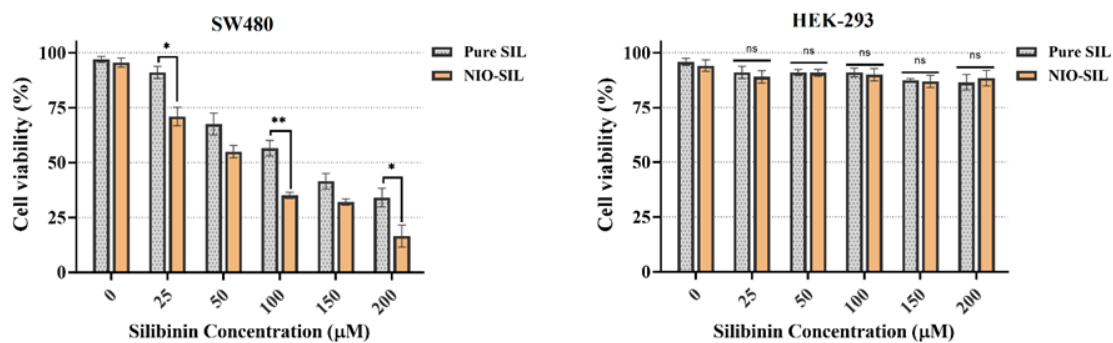


Figure 6. *In vitro* Cytotoxicity Analysis by MTT. The viability of SW480 and HEK-293 cells after incubation with pure silibinin and silibinin-loaded PEGylated niosome NPs after 48 h treatment. (*P value < 0.05, **P value < 0.001)

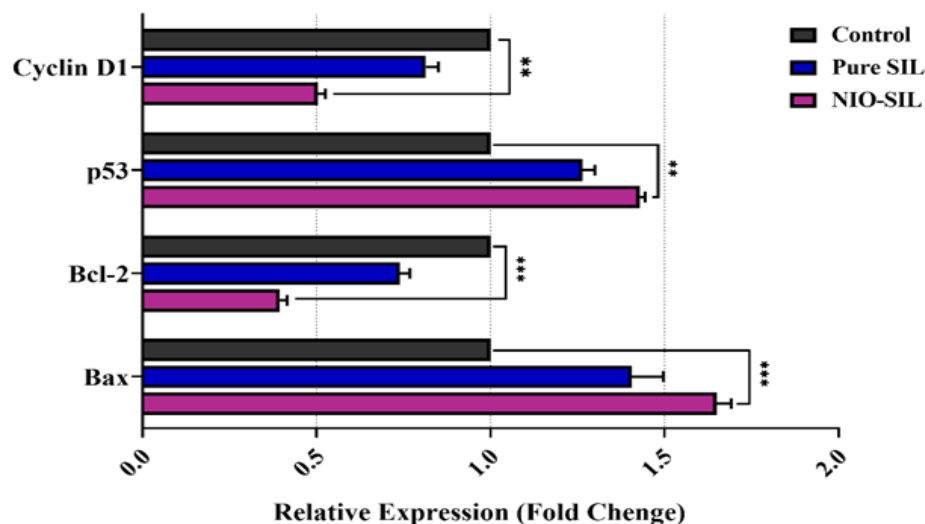


Figure 7. Changes in Expression Level of Bax, Bcl-2, p53, and Cyclin D1 Genes in Human Cancerous Cells Treated with Pure Silibinin and Silibinin-Loaded PEGylated Niosome NPs after 48 h Treatment. (p value < 0.001 *** and p value < 0.01 **).

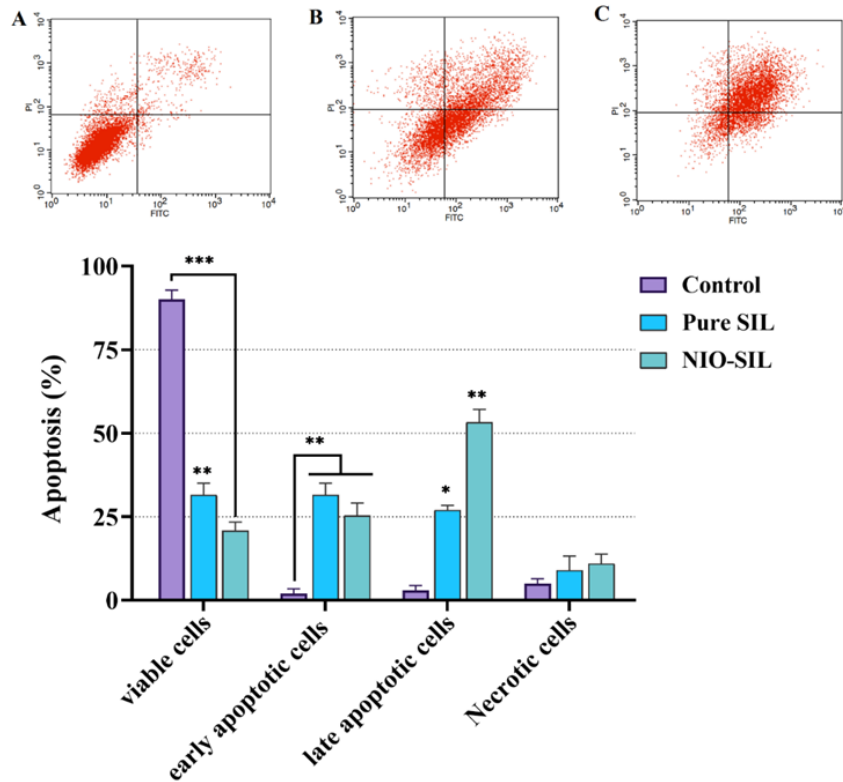


Figure 8. Identification of Apoptosis Using the Flow Cytometric Assay (Annexin V/PI staining). (A) Control group, (B) treated SW480 cells with pure silibinin, and (C) treated SW480 cells with silibinin-loaded PEGylated niosome NPs after 48 hours. (p-value < 0.001 ***, p-value < 0.01 **, and p-value < 0.05 *).

microscopic images of NIO-SIL NPs obtained with SEM. These NPs have mostly spherical morphology, which is consistent with previous studies. Figure 3 illustrates the AFM image of NIO-SIL NPs with good dispersion and no aggregation.

Discussion

Drug release in nanoparticles (NPs) is a critical aspect of their functionality, impacting their therapeutic efficacy and toxicity in vivo [56]. The release profile of drugs from NPs is influenced by various factors, including the physicochemical characteristics of the NPs [56]. For instance, the initial burst release from NPs can be

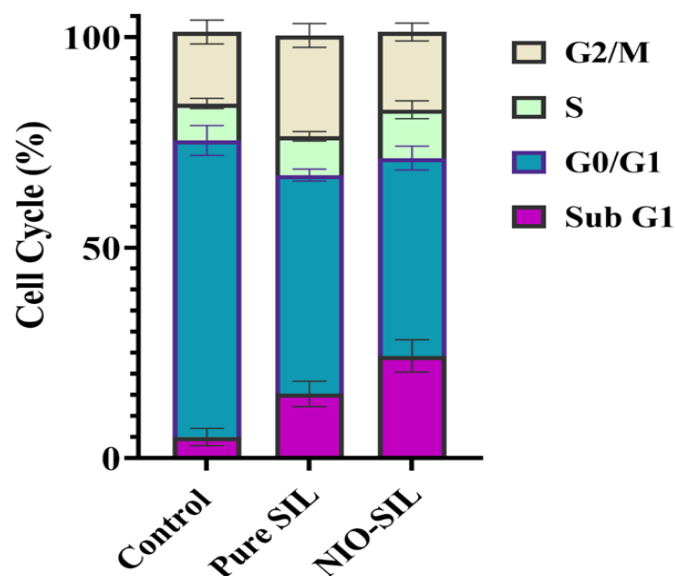


Figure 9. Suppression Effects of Pure Silibinin and Silibinin-Loaded PEGylated Niosome NPs on the Cell Cycle of SW480 Cells. Treatment with pure silibinin and silibinin-loaded PEGylated niosome NPs causes cell cycle arrest at the Sub G1 phase.

attributed to the immediate desorption of drug molecules adsorbed onto the particle surface, as well as the shorter average diffusion path due to the nanoscale of the NPs, leading to rapid drug molecule release [57]. Figure 4 demonstrates the 96-hour drug release profile of NIO-SIL in human physiological pH (7.4) and cancerous cell cytoplasmic pH (5). It shows a cumulative profile that follows two distinct phases in both pH. As mentioned above, the initial burst release of silibinin from niosome NPs can result from the immediate desorption of silibinin molecules adsorbed onto the niosome surface.

Encapsulation efficiency is another factor in the development of carriers and delivery systems. It is defined as the ratio of the quantity of encapsulated material to the total quantity initially added, and it is a key indicator of the effectiveness of the encapsulation process. Higher encapsulation efficiency is desirable because it ensures that a greater amount of the drug is successfully encapsulated within the NPs, resulting in enhanced drug delivery and therapeutic outcome [58]. The encapsulation efficiency of NiO-SiL NPs was found to be 76.4%, indicating a significant loading effectiveness.

In Figure 5, the spectrum of pure silibinin shows a distinct absorption peak at 3452 cm^{-1} , which is attributed to the $-\text{OH}$ stretching vibration [59]. Additionally, the pure silibinin spectrum shows increased absorbance in the carbonyl band at 1642.9 cm^{-1} , indicating the presence of the ring ketonic group in silibinin [60]. The cholesterol spectrum exhibited distinctive peaks corresponding to methylene rocking at 802 cm^{-1} , C–O stretching at 1055 cm^{-1} , C–H bond stretching in the range of 2800–3000 cm^{-1} , C–H bond bending at 1376 cm^{-1} , and $-\text{OH}$ stretching with a broad peak spanning 3100–3600 cm^{-1} . In contrast, Span 60 manifested peaks indicative of C=O stretching at 1738 cm^{-1} , $-\text{C}-\text{CO}-\text{O}-$ at 1171 cm^{-1} , aliphatic CH stretching (asymmetric and symmetric at 2916 cm^{-1} and 2849 cm^{-1} , respectively), and aliphatic $-\text{CH}_2-$ rocking at 722 cm^{-1} [61]. The NIO-SIL NPs FTIR spectra featured characteristic peaks corresponding to pure silibinin, cholesterol, Span 60, and PEG, affirming the lack of discernible chemical interactions among them.

The MTT assay, based on the reduction of (4,5-Dimethylthiazol-2-yl)-2,5-diphenyltetrazolium bromide (MTT) to formazan by living cells, is a widely used method for measuring cell viability and proliferation [62]. This assay determines mitochondrial activity and is utilized to assess cell survival, proliferation, and cytotoxicity [63]. It has been used to evaluate the effects of different compounds on cell viability and proliferation [64]. Figure 6 illustrates the cytotoxic effects of pure silibinin and NIO-SIL NPs on the human normal cell line (HEK-293) and the human colon cancer cell line (SW480). The pure silibinin shows toxicity on cancerous cells at different concentrations; however, it slightly inhibits the proliferation of normal cells at the highest concentration. The results of NIO-SIL NPs demonstrate enhanced effects of silibinin when using PEGylated niosomal NPs as carriers against SW480 cells. The results of NIO-SIL nanoparticles show significantly improved effects of silibinin when using PEGylated niosomal NPs as a carrier against cancer cells at concentrations of 25,

100, and 200 μM . As evident, NIO-SIL NPs show better results than pure silibinin even at lower concentrations. The remarkable point is the non-toxicity of NIO-SIL NPs on normal human cells. Considering that lower concentrations of silibinin were used in NIO-SIL NPs, these results can be justified. Based on the obtained results, the blank NIO NPs were excluded from further tests due to their insignificant toxicity towards cell lines and pure silibinin and NIO-SIL were used at their IC_{50} concentrations for next tests.

Gene expression analysis is a tool utilized to comprehend the underlying mechanisms of biological processes and complex diseases. It involves the identification of expressed genes. Determining their level of expression under different circumstances. In this study (Figure 7), we assessed the expression of *Bax*, *Bcl-2*, *p53*, and *Cyclin D1* genes using real-time PCR. *Bax* is a protein belonging to the *Bcl-2* family of proteins. It plays a role in regulating apoptosis in both cancer cells. The activation of *Bax* leads to membrane permeabilization, which subsequently results in the release of cytochrome c and eventual cell death in cancer cells [65, 66]. Quantifying *Bax* protein levels can provide valuable information for cancer treatment and research, as it is closely associated with drug resistance in tumor cells [67]. Studies have demonstrated that colorectal cancer tissues typically exhibit increased *Bax* expression. Its absence can lead to reduced proliferation and colony formation ability in cancer cells [68]. On the other hand, *Bcl-2* is a gene that significantly influences the regulation of apoptosis, or programmed cell death, in cancer cells. Aberrant expression of the *Bcl-2* gene strongly correlates with chemotherapy and radiation resistance, contributing to tumorigenesis while promoting cell survival [69, 70]. The *Bcl-2* protein family is composed of members that can either promote or prevent cell death, working together to maintain an equilibrium in cells [69]. In the realm of cancer, *p53* is a protein that possesses the ability to regulate cellular processes such as the cell cycle, DNA repair, and programmed cell death [71]. Mutations in the TP53 gene, which encodes *p53*, can result in the loss or gain of tumor-suppressor function [72]. The results show a decrease in the expression of the *Bcl-2* and *Cyclin D1* genes and an overexpression of the *bax* and *p53* genes in both silibinin-treated and NIO-SIL-treated cells. However, these changes in gene expression are more evident in NIO-Sil treated cells compared to other cells. As mentioned earlier, this can be achieved due to the enhanced effects of silibinin when using PEGylated niosomal NPs as a carrier against cancer cells.

Apoptosis, also known as programmed cell death, is a highly regulated process crucial for various physiological events, including development, tissue homeostasis, and immune response [73]. It involves a series of signaling pathways that can be broadly categorized into intrinsic and extrinsic pathways. The intrinsic pathway is triggered by intracellular stresses, leading to the release of pro-apoptotic factors from mitochondria, while the extrinsic pathway is initiated by external signals binding to death receptors on the cell surface [74]. Previous studies have confirmed the apoptotic effects of silibinin on breast [75], lung [76], pancreatic [77] and other cancers.

Figure 8 shows the induction of apoptosis in SW480 cells with pure silibinin and NIO-SIL NPs. The NIO-SIL NPs could significantly reduce amount of viable cell at 24 hours of treatment. Both pure silibinin and NIO-SIL NPs induce early and late apoptosis in cancerous cells.

The cell cycle is a highly regulated process involving a series of events that lead to cell division. It is controlled by a complex interplay of intracellular and extracellular signals [75]. Key regulators of the cell cycle include cyclin-dependent kinases and cyclins, which coordinate various phases of the cycle [78]. As demonstrated in Figure 9, the untreated SW480 cells (control cells) are mostly in the G0/G1 phase. After 24 hours of treatment with pure silibinin and NIO-SIL NPs, a shift in these cells to the Sub G1 phase occurs. The G0/G1 to sub-G1 cycle is controlled by cyclin D1 expression. These results are consistent with the RT-PCR findings, which confirmed a reduction in the expression of the cyclin D1 gene, leading to cell cycle arrest at the Sub-G1 phase. In this study, silibinin was applied as a therapeutic agent against human colorectal cancer cells. The research involved evaluating cell proliferation and examining the expression of pivotal cancer-associated genes such as bax, bcl-2, and p53. To overcome the issue of silibinin's restricted solubility, a PEGylated-niosomal nanoparticle (NPs) platform was devised to improve its delivery efficiency. Future investigations will explore additional types of colon cancer cells and other pathways implicated in cancer advancement.

In conclusion, in this study, PEGylated niosomal NPs fabricated using the thin-film hydration method were employed as carriers for the delivery of silibinin into colorectal cancer cells (SW480). Based on our results, the fabricated PEGylated niosomal NPs have no negative effects on the proliferation of human normal cells. Furthermore, nano-delivery of silibinin could reduce the proliferation of SW480 cancer cells more effectively than pure silibinin at the same dosage. These results highlight the promising effects of PEGylated-niosomal NPs as a nanodrug delivery system. We hope that this work will lay the scientific foundation for future clinical trials of nanotherapy using silibinin for the treatment of colorectal cancer.

Author Contribution Statement

Urjwan Abdul Jabbar Ridha: Methodology, Investigation, Data curation, Original draft preparation. Maha Mohammed Kadhim Al-Tu'ma: Methodology, Investigation, Data curation, Original draft preparation. Ammar Fadhil Jawad: Original draft preparation, Reviewing and editing. Saja Talib Ahmed: Reviewing and editing. Hanaa Addai Ali: Reviewing and editing. Fadhil Jawad Al-Tu'ma: Supervision, Conceptualization, Writing- Reviewing and Editing.

Acknowledgements

Availability of data and materials

The data and materials that support the findings of this study are available from the corresponding author, upon

reasonable request.

Conflict of interest

The authors declare that they have no conflict of interests.

References

- Calonge N, Petitti DB, DeWitt TG, Dietrich AJ, Gregory KD, Harris R, et al. Screening for colorectal cancer: Us preventive services task force recommendation statement. *Ann Internal Med.* 2008;149(9):627-37.
- Koh M, Kim M-C, Jang JS. Difference in the prevalence of advanced colon adenoma between patients with gastric neoplasm and healthy people: A strobe-compliant study. *Medicine.* 2022;101(21). <https://doi.org/10.1097/MD.00000000000029308>.
- Magar CBP, Bhatta RR, Pandey G, Uprety S, Dhungana I, Jha N. An overview of colorectal cancer in tertiary care cancer center of nepal. *Nepal Med J.* 2022;6(2):40-5.
- Sato A, Matsubayashi K, Morishima T, Nakata K, Kawakami K, Miyashiro I. Increasing trends in the prevalence of prior cancer in newly diagnosed lung, stomach, colorectal, breast, cervical, and corpus uterine cancer patients: A population-based study. *BMC Cancer.* 2021;21(1):264. <https://doi.org/10.1186/s12885-021-08011-3>.
- Sheffer M, Bacolod MD, Zuk O, Giardina SF, Pincas H, Barany F, et al. Association of survival and disease progression with chromosomal instability: A genomic exploration of colorectal cancer. *Proc Natl Acad Sci U S A.* 2009;106(17):7131-6. <https://doi.org/10.1073/pnas.0902232106>.
- Nakao K, Mehta KR, Fridlyand J, Moore DH, Jain AN, Lafuente A, et al. High-resolution analysis of DNA copy number alterations in colorectal cancer by array-based comparative genomic hybridization. *Carcinogenesis.* 2004;25(8):1345-57. <https://doi.org/10.1093/carcin/bgh134>.
- Grabsch H, Dattani M, Barker L, Maughan N, Maude K, Hansen O, et al. Expression of DNA double-strand break repair proteins atm and brca1 predicts survival in colorectal cancer. *Clin Cancer Res.* 2006;12(5):1494-500. <https://doi.org/10.1158/1078-0432.CCR-05-2105>.
- Postma C, Hermsen MA, Coffa J, Baak JP, Mueller JD, Mueller E, et al. Chromosomal instability in flat adenomas and carcinomas of the colon. *J Pathol.* 2005;205(4):514-21. <https://doi.org/10.1002/path.1733>.
- Verdura S, Cuyas E, Ruiz-Torres V, Micol V, Joven J, Bosch-Barrera J, et al. Lung cancer management with silibinin: A historical and translational perspective. *Pharmaceuticals (Basel).* 2021;14(6):559. <https://doi.org/10.3390/ph14060559>.
- Xu S, Zhang H, Wang A, Ma Y, Gan Y, Li G. Silibinin suppresses epithelial-mesenchymal transition in human non-small cell lung cancer cells by restraining rhbddd1. *Cell Mol Biol Lett.* 2020;25(1):36. <https://doi.org/10.1186/s11658-020-00229-6>.
- Xu R, Qiu S, Zhang J, Liu X, Zhang L, Xing H, et al. Silibinin schiff base derivatives counteract ccl4-induced acute liver injury by enhancing anti-inflammatory and antiapoptotic bioactivities. *Drug Des Devel Ther.* 2022;1441-56. <https://doi.org/10.2147/DDDT.S356847>.
- Sun X, Ping Y, Li X, Mao Y, Chen Y, Shi L, et al. Activation of pgc-1alpha-dependent mitochondrial biogenesis supports therapeutic effects of silibinin against type i diabetic periodontitis. *J Clin Periodontol.* 2023;50(7):964-79. <https://doi.org/10.1111/jcpe.13811>.

13. Lashgarian HE, Adamii V, Ghorbanzadeh V, Chodari L, Kamali F, Akbari S, et al. Silibinin inhibit cell migration through downregulation of rac1 gene expression in highly metastatic breast cancer cell line. *Drug Res.* 2020;70(10):478-83. <https://doi.org/10.1055/a-1223-1734>.
14. Bosch-Barrera J, Verdura S, Ruffinelli JC, Carcereny E, Sais E, Cuyas E, et al. Silibinin suppresses tumor cell-intrinsic resistance to nintedanib and enhances its clinical activity in lung cancer. *Cancers (Basel).* 2021;13(16):4168. <https://doi.org/10.3390/cancers13164168>.
15. Zhang Y, Ge Y, Ping X, Yu M, Lou D, Shi W. Synergistic apoptotic effects of silibinin in enhancing paclitaxel toxicity in human gastric cancer cell lines. *Mol Med Rep.* 2018;18(2):1835-41. <https://doi.org/10.3892/mmr.2018.9129>.
16. Dupuis ML, Conti F, Maselli A, Pagano MT, Ruggieri A, Anticoli S, et al. The natural agonist of estrogen receptor beta silibinin plays an immunosuppressive role representing a potential therapeutic tool in rheumatoid arthritis. *Front Immunol.* 2018;9:1903. <https://doi.org/10.3389/fimmu.2018.01903>.
17. Majeed AAA, Sahib AS, Mahmood HS, Mohsin KK, Abbas RF. Association of cytidine deaminase polymorphism with capecitabine effectiveness in breast cancer patients. *Asian Pac J Cancer Prev.* 2023;24(12):4219. <https://doi.org/10.31557/APJCP.2023.24.12.4219>.
18. Ravi R, Zeyaulah M, Ghosh S, Khan Warsi M, Baweja R, AlShahrani AM, et al. Use of gold nanoparticle-silibinin conjugates: A novel approach against lung cancer cells. *Front Chem.* 2022;10:1018759. <https://doi.org/10.3389/fchem.2022.1018759>.
19. Han HS, Koo SY, Choi KY. Emerging nanoformulation strategies for phytochemicals and applications from drug delivery to phototherapy to imaging. *Bioact Mater.* 2022;14:182-205. <https://doi.org/10.1016/j.bioactmat.2021.11.027>.
20. Hadi ZA, Odda AH, Jawad AF, Al-Tu'ma FJ. Design and development of Fe₃O₄@ Prussian blue nanocomposite: Potential application in the detoxification of bilirubin. *Asian Pac J Cancer Prev.* 2023;24(8):2809. <https://doi.org/10.31557/APJCP.2023.24.8.2809>.
21. Rad AH, Asiaee F, Jafari S, Shayanfar A, Lavasanifar A, Molavi O. Poly (ethylene glycol)-poly (ϵ -caprolactone)-based micelles for solubilization and tumor-targeted delivery of silibinin. *BioImpacts.* 2020;10(2):87. <https://doi.org/10.34172/bi.2020.11>.
22. Hossainzadeh S, Ranji N, Naderi Sohi A, Najafi F. Silibinin encapsulation in polymersome: A promising anticancer nanoparticle for inducing apoptosis and decreasing the expression level of mir-125b/mir-182 in human breast cancer cells. *J Cell Physiol.* 2019;234(12):22285-98. <https://doi.org/10.1002/jcp.28795>.
23. Kumavat S, Sharma PK, Koka SS, Sharma R, Gupta A, Darwhekar G. A review on niosomes: Potential vesicular drug delivery system. *J Drug Deliv Ther.* 2021;11(5):208-12. <https://doi.org/10.22270/jddt.v11i5.5046>.
24. Kim H, Jang H, Cho H, Choi J, Hwang KY, Choi Y, et al. Recent advances in exosome-based drug delivery for cancer therapy. *Cancers (Basel).* 2021;13(17):4435. <https://doi.org/10.3390/cancers13174435>.
25. Jadid MFS, Jafari-Gharabaghrou D, Bahrami MK, Bonabi E, Zarghami N. Enhanced anti-cancer effect of curcumin loaded-niosomal nanoparticles in combination with heat-killed *Saccharomyces cerevisiae* against human colon cancer cells. *Int J Drug Deliv Technol.* 2023;80:104167.
26. Shafiei G, Jafari-Gharabaghrou D, Farhoudi-Sefidan-Jadid M, Alizadeh E, Fathi M, Zarghami N. Targeted delivery of silibinin via magnetic niosomal nanoparticles: Potential application in treatment of colon cancer cells. *Front Pharmacol.* 2023;14:1174120. <https://doi.org/10.3389/fphar.2023.1174120>.
27. Hoang Thi TT, Pilkington EH, Nguyen DH, Lee JS, Park KD, Truong NP. The importance of poly(ethylene glycol) alternatives for overcoming peg immunogenicity in drug delivery and bioconjugation. *Polymers (Basel).* 2020;12(2):298. <https://doi.org/10.3390/polym12020298>.
28. Zuma LK, Gasa NL, Makhoba XH, Poee OJ. Protein pegylation: Navigating recombinant protein stability, aggregation, and bioactivity. *Biomed Res Int.* 2022;2022:8929715. <https://doi.org/10.1155/2022/8929715>.
29. Zare Kazemabadi F, Heydarinasab A, Akbarzadeh A, Ardjmand M. Preparation, characterization and in vitro evaluation of pegylated nanoliposomal containing etoposide on lung cancer. *Artif Cells Nanomed Biotechnol.* 2019;47(1):3222-30. <https://doi.org/10.1080/21691401.2019.1646265>.
30. Alemi A, Zavar Reza J, Haghirsadat F, Zarei Jalani H, Haghi Karamallah M, Hosseini SA, et al. Paclitaxel and curcumin coadministration in novel cationic pegylated niosomal formulations exhibit enhanced synergistic antitumor efficacy. *J Nanobiotechnology.* 2018;16(1):28. <https://doi.org/10.1186/s12951-018-0351-4>.
31. Saharkhiz S, Zarepour A, Zarrabi A. Empowering cancer therapy: Comparing pegylated and non-pegylated niosomes loaded with curcumin and doxorubicin on mcf-7 cell line. *Bioengineering (Basel).* 2023;10(10):1159. <https://doi.org/10.3390/bioengineering10101159>.
32. Salmani-Javan E, Jafari-Gharabaghrou D, Bonabi E, Zarghami N. Fabricating niosomal-peg nanoparticles co-loaded with metformin and silibinin for effective treatment of human lung cancer cells. *Front Oncol.* 2023;13:1193708. <https://doi.org/10.3389/fonc.2023.1193708>.
33. Barani M, Mirzaei M, Torkzadeh-Mahani M, Lohrasbi-Nejad A, Nematollahi MH. A new formulation of hydrophobin-coated niosome as a drug carrier to cancer cells. *Mater Sci Eng C Mater Biol Appl.* 2020;113:110975. <https://doi.org/10.1016/j.msec.2020.110975>.
34. Es-haghi A, Javadi F, Yazdi MET, Amiri MS. The expression of antioxidant genes and cytotoxicity of biosynthesized cerium oxide nanoparticles against hepatic carcinoma cell line. *Avicenna J Med Biochem.* 2019;7(1):16-20. <https://doi.org/10.34172/ajmb.2019.04>.
35. Al-Kinani MA, Haider AJ, Al-Musawi S. Design and synthesis of nanoencapsulation with a new formulation of Fe@ Au-CS-Cu-fa nps by pulsed laser ablation in liquid (plal) method in breast cancer therapy: In vitro and in vivo. *Plasmonics.* 2021;16(4):1107-17. <https://doi.org/10.1007/s11468-021-01371-3>.
36. Sun M, Wang T, Li L, Li X, Zhai Y, Zhang J, et al. The application of inorganic nanoparticles in molecular targeted cancer therapy: Egfr targeting. *Front Pharmacol.* 2021;12:702445. <https://doi.org/10.3389/fphar.2021.702445>.
37. Gavas S, Quazi S, Karpinski TM. Nanoparticles for cancer therapy: Current progress and challenges. *Nanoscale Res Lett.* 2021;16(1):173. <https://doi.org/10.1186/s11671-021-03628-6>.
38. Chen M, Shou Z, Jin X, Chen Y. Emerging strategies in nanotechnology to treat respiratory tract infections: Realizing current trends for future clinical perspectives. *Drug Deliv.* 2022;29(1):2442-58. <https://doi.org/10.1080/10717544.2022.2089294>.
39. Peer D, Karp JM, Hong S, Farokhzad OC, Margalit R, Langer R. Nanocarriers as an emerging platform for cancer therapy. *Nano-enabled medical applications.* 2020:61-91. <https://doi.org/10.1016/j.nano.2020.01.001>.

- org/10.1038/nano.2007.387.
40. El-Far SW, Abo El-Enin HA, Abdou EM, Nafea OE, Abdelmonem R. Targeting colorectal cancer cells with niosomes systems loaded with two anticancer drugs models; comparative in vitro and anticancer studies. *Pharmaceuticals (Basel)*. 2022;15(7):816. <https://doi.org/10.3390/ph15070816>.
 41. Yadav R, Chanana A, Chawra HS, Pal R. Recent advances in niosomal drug delivery: A review. *Int J Multidiscip Res*.5(1). <https://doi.org/10.3390/ijms12084861>.
 42. Kondiah PPD, Rants'o TA, Mdanda S, Mohlomi LM, Choonara YE. A poly (caprolactone)-cellulose nanocomposite hydrogel for transdermal delivery of hydrocortisone in treating psoriasis vulgaris. *Polymers (Basel)*. 2022;14(13):2633. <https://doi.org/10.3390/polym14132633>.
 43. Alnaim AS, Shah H, Nair AB, Mewada V, Patel S, Jacob S, et al. Qbd-based approach to optimize niosomal gel of levosulpiride for transdermal drug delivery. *Gels*. 2023;9(3):213. <https://doi.org/10.3390/gels9030213>.
 44. Miatmoko A, Safitri SA, Aquila F, Cahyani DM, Hariawan BS, Hendrianto E, et al. Characterization and distribution of niosomes containing ursolic acid coated with chitosan layer. *Res Pharm Sci*. 2021;16(6):660-73. <https://doi.org/10.4103/1735-5362.327512>.
 45. Iskandarsyah I, Masrijal CDP, Harmita H. Effects of sonication on size distribution and entrapment of lymestrenol transferosome. *Int J App Pharm*. 2020:245-7.
 46. Barani M, Reza Hajinezhad M, Sargazi S, Zeeshan M, Rahdar A, Pandey S, et al. Simulation, in vitro, and in vivo cytotoxicity assessments of methotrexate-loaded ph-responsive nanocarriers. *Polymers (Basel)*. 2021;13(18):3153. <https://doi.org/10.3390/polym13183153>.
 47. Obeid MA, Gany SAS, Gray AI, Young L, Igoli JO, Ferro VA. Niosome-encapsulated balanocarpol: Compound isolation, characterisation, and cytotoxicity evaluation against human breast and ovarian cancer cell lines. *Nanotechnology*. 2020;31(19):195101. <https://doi.org/10.1088/1361-6528/ab6d9c>.
 48. Haddadian A, Robattorki FF, Dibah H, Soheili A, Ghanbarzadeh E, Sartipnia N, et al. Niosomes-loaded selenium nanoparticles as a new approach for enhanced antibacterial, anti-biofilm, and anticancer activities. *Sci Rep*. 2022;12(1):21938. <https://doi.org/10.1038/s41598-022-26400-x>.
 49. De Silva L, Fu JY, Htar TT, Muniyandy S, Kasbollah A, Wan Kamal WHB, et al. Characterization, optimization, and in vitro evaluation of technetium-99m-labeled niosomes. *Int J Nanomedicine*. 2019;14:1101-17. <https://doi.org/10.2147/IJN.S184912>.
 50. Khan R, Irchhaiya R. In vitro in vivo evaluation of niosomal formulation of famotidine. *Int J Pharm Pharm Sci*. 2020. <https://doi.org/10.22159/ijpps.2020v12i3.36210>.
 51. Al Mahrouqi D, Vinogradov J, Jackson MD. Zeta potential of artificial and natural calcite in aqueous solution. *Adv Colloid Interface Sci*. 2017;240:60-76. <https://doi.org/10.1016/j.cis.2016.12.006>.
 52. Teo YY, Misran M, Low KH, Zain SM. Effect of unsaturation on the stability of c-18 polyunsaturated fatty acids vesicles suspension in aqueous solution. *B Korean Chem Soc*. 2011;32(1):59-64. <https://doi.org/10.5012/bkcs.2011.32.1.59>.
 53. Zare-Zardini H, Alemi A, Taheri-Kafrani A, Hosseini SA, Soltaninejad H, Hamidieh AA, et al. Assessment of a new ginsenoside rh2 nanoniosomal formulation for enhanced antitumor efficacy on prostate cancer: An in vitro study. *Drug Des Devel Ther*. 2020;14:3315-24. <https://doi.org/10.2147/DDDT.S261027>.
 54. Rampersaud S, Fang J, Wei Z, Fabijanic K, Silver S, Jaikaran T, et al. The effect of cage shape on nanoparticle-based drug carriers: Anticancer drug release and efficacy via receptor blockade using dextran-coated iron oxide nanocages. *Nano Lett*. 2016;16(12):7357-63. <https://doi.org/10.1021/acs.nanolett.6b02577>.
 55. Durak S, Esmaceli Rad M, Alp Yetisgin A, Eda Sutova H, Kutlu O, Cetinel S, et al. Niosomal drug delivery systems for ocular disease-recent advances and future prospects. *Nanomaterials (Basel)*. 2020;10(6):1191. <https://doi.org/10.3390/nano10061191>.
 56. Morgulchik N, Kamaly N. Meta-analysis of in vitro drug-release parameters reveals predictable and robust kinetics for redox-responsive drug-conjugated therapeutic nanogels. *ACS Appl Nano Mater*. 2021;4(5):4256-68. <https://doi.org/10.1021/acsanm.1c00170>.
 57. Hu H, Liao Z, Xu M, Wan S, Wu Y, Zou W, et al. Fabrication, optimization, and evaluation of paclitaxel and curcumin coloaded plga nanoparticles for improved antitumor activity. *ACS Omega*. 2023;8(1):976-86. <https://doi.org/10.1021/acsomega.2c06359>.
 58. Vulić J, Ranitović A, Tumbas-Šaponjac V, Četković G, Čanadanović-Brunet J, Cvetković D, et al. Microencapsulation of beetroot pomace extractin cells of *saccharomyces cerevisiae*. *Chem Ind Chem Eng*. 2019;25(4):321-7. <https://doi.org/10.2298/CICEQ181003011V>.
 59. Tan JM, Karthivashan G, Arulselvan P, Fakurazi S, Hussein MZ. Characterization and in vitro sustained release of silibinin from ph responsive carbon nanotube-based drug delivery system. *J Nanomater*. 2014;2014:1-. <https://doi.org/10.1155/2014/439873>.
 60. Undre SB, Singh M, Kale R, Rizwan M. Silibinin binding and release activities moderated by interstices of trimesoyl, tridimethyl, and tri-diethyl malonate first-tier dendrimers. *J Appl Polym Sci*. 2013;130(5):3537-54. <https://doi.org/10.1002/app.39466>.
 61. Farmoudeh A, Akbari J, Saeedi M, Ghasemi M, Asemi N, Nokhodchi A. Methylene blue-loaded niosome: Preparation, physicochemical characterization, and in vivo wound healing assessment. *Drug Deliv Transl Res*. 2020;10(5):1428-41. <https://doi.org/10.1007/s13346-020-00715-6>.
 62. Liu Y, Peterson DA, Kimura H, Schubert D. Mechanism of cellular 3-(4,5-dimethylthiazol-2-yl)-2,5-diphenyltetrazolium bromide (mtt) reduction. *J Neurochem*. 1997;69(2):581-93. <https://doi.org/10.1046/j.1471-4159.1997.69020581.x>.
 63. Liu CW, Sung HC, Lin SR, Wu CW, Lee CW, Lee IT, et al. Resveratrol attenuates icam-1 expression and monocyte adhesiveness to tnf-alpha-treated endothelial cells: Evidence for an anti-inflammatory cascade mediated by the mir-221/222/ampk/p38/nf-kappab pathway. *Sci Rep*. 2017;7(1):44689. <https://doi.org/10.1038/srep44689>.
 64. Kumar KH, Khanum F. Hydroalcoholic extract of cyperus rotundus ameliorates h 2 o 2-induced human neuronal cell damage via its anti-oxidative and anti-apoptotic machinery. *Cell Mol Neurobiol*. 2013;33:5-17. <https://doi.org/10.1007/s10571-012-9865-8>.
 65. Liu Z, Ding Y, Ye N, Wild C, Chen H, Zhou J. Direct activation of bax protein for cancer therapy. *Med Res Rev*. 2016;36(2):313-41. <https://doi.org/10.1002/med.21379>.
 66. Al-Tu'ma FJ, Al-Zubaidi RD, Al-Khaleeli A-MB, Abo-Almaali HM. Polymorphism of tumor suppressor gene (p53) codon 72 in iraqi patients with acute myocardial infarction. *J Contemp Med Sci*. 2016;2(7):74-6.
 67. Xu L, Zhu L, Jia N, Huang B, Tan L, Yang S, et al. Quantification of bax protein on tumor cells based on electrochemical immunoassay. *Sens Actuators B Chem*.

- 2013;186:506-14. <https://doi.org/10.1016/j.snb.2013.06.047>
68. Su L, Suyila Q, Yang L, Li H, Xi Y, Su X. *Bax* is involved in the anticancer activity of velcade in colorectal cancer. *Exp Ther Med*. 2017;14(4):3179-83. <https://doi.org/10.3892/etm.2017.4857>.
69. Knight T, Luedtke D, Edwards H, Taub JW, Ge Y. A delicate balance - the *bcl-2* family and its role in apoptosis, oncogenesis, and cancer therapeutics. *Biochem Pharmacol*. 2019;162:250-61. <https://doi.org/10.1016/j.bcp.2019.01.015>.
70. Zhang L, Lu Z, Zhao X. Targeting *bcl-2* for cancer therapy. *Biochim Biophys Acta Rev Cancer*. 2021;1876(1):188569. <https://doi.org/10.1016/j.bbcan.2021.188569>.
71. Ozaki T, Nakagawara A. Role of *p53* in cell death and human cancers. *Cancers (Basel)*. 2011;3(1):994-1013. <https://doi.org/10.3390/cancers3010994>.
72. Pavlakis E, Stiewe T. P53's extended reach: The mutant *p53* secretome. *Biomolecules*. 2020;10(2):307. <https://doi.org/10.3390/biom10020307>.
73. Chowdhury I, Tharakan B, Bhat GK. Current concepts in apoptosis: The physiological suicide program revisited. *Cell Mol Biol Lett*. 2006;11(4):506-25. <https://doi.org/10.2478/s11658-006-0041-3>.
74. Hong JY, Kim GH, Kim JW, Kwon SS, Sato EF, Cho KH, et al. Computational modeling of apoptotic signaling pathways induced by cisplatin. *BMC Syst Biol*. 2012;6:122. <https://doi.org/10.1186/1752-0509-6-122>.
75. Si L, Liu W, Hayashi T, Ji Y, Fu J, Nie Y, et al. Silibinin-induced apoptosis of breast cancer cells involves mitochondrial impairment. *Arch Biochem Biophys*. 2019;671:42-51. <https://doi.org/10.1016/j.abb.2019.05.009>.
76. Rugamba A, Kang DY, Sp N, Jo ES, Lee JM, Bae SW, et al. Silibinin regulates tumor progression and tumorsphere formation by suppressing *pd-l1* expression in non-small cell lung cancer (nscle) cells. *Cells*. 2021;10(7):1632. <https://doi.org/10.3390/cells10071632>.
77. Ge Y, Zhang Y, Chen Y, Li Q, Chen J, Dong Y, et al. Silibinin causes apoptosis and cell cycle arrest in some human pancreatic cancer cells. *Int J Mol Sci*. 2011;12(8):4861-71. <https://doi.org/10.3390/ijms12084861>.
78. Dephoure N, Zhou C, Villen J, Beausoleil SA, Bakalarski CE, Elledge SJ, et al. A quantitative atlas of mitotic phosphorylation. *Proc Natl Acad Sci U S A*. 2008;105(31):10762-7. <https://doi.org/10.1073/pnas.0805139105>.



This work is licensed under a Creative Commons Attribution-Non Commercial 4.0 International License.